Earth and Planetary Science Letters 474 (2017) 226–236

Contents lists available at ScienceDirect

Earth and Planetary Science Letters

www.elsevier.com/locate/epsl

Mapping the mantle transition zone beneath Hawaii from Ps receiver functions: Evidence for a hot plume and cold mantle downwellings

Matthew R. Agius [a,*], Catherine A. Rychert [a], Nicholas Harmon [a], Gabi Laske [b]

[a] Ocean and Earth Science, University of Southampton, United Kingdom
[b] Scripps Institution of Oceanography, University of California, San Diego, CA, USA

ARTICLE INFO

Article history:
Received 16 February 2017
Received in revised form 27 May 2017
Accepted 19 June 2017
Available online xxxx
Editor: R. Bendick

Keywords:
Hawaii
seismology
mantle plume
transition zone
mantle discontinuities
receiver functions

ABSTRACT

Hawaii is the archetypal example of hotspot volcanism. Classic plume theory suggests a vertical plume ascent from the core–mantle boundary to the surface. However, recently it has been suggested that the plume path may be more complex. Determining the exact trajectory of the Hawaiian plume seismic anomaly in the mantle has proven challenging. We determine P-to-S (Ps) receiver functions to illuminate the 410- and 660-km depth mantle discontinuities beneath the Hawaiian Islands using waveforms recorded on land and ocean-bottom seismometers, applying new corrections for tilt and coherence to the ocean bottom data. Our 3-D depth-migrated maps provide enhanced lateral resolution of the mantle transition zone discontinuities. The 410 discontinuity is characterised by a deepened area beneath central Hawaii, surrounded by an elevated shoulder. At the 660 discontinuity, shallow topography is located to the north and far south of the islands, and a deep topographic anomaly is located far west and east. The transition zone thickness varies laterally by ±13 km depth: thin beneath north-central Hawaii and thick farther away in a horseshoe-like feature. We infer that at 660-km depth a broad or possibly a double region of upwelling converges into a single plume beneath central Hawaii at 410-km depth. As the plume rises farther, uppermost mantle melting and flow results in the downwelling of cold material, down to at least 410 km surrounding the plume stem. This result in the context of others supports complex plume dynamics including a possible non-vertical plume path and adjacent mantle downwellings.

1. Introduction

In classical plume theory, mantle material rises vertically from the lowermost mantle to the surface of the Earth (Morgan, 1972). This theory was inspired by linear, age-progressive volcanic tracks trending in the direction of past and present plate motions such as the Hawaiian–Emperor seamount chain, which suggest that plate motion is over a fixed mantle upwelling (Wilson, 1963). Geochemical isotopes suggest that ocean-island volcanism may originate from a distinct mantle reservoir at the base of the mantle (e.g., Hofmann, 1997). Global seismic tomography studies image vertically elongated low-velocity anomalies associated with the ascending hot mantle through the entire lower mantle (e.g., Zhao, 2015; French and Romanowicz, 2015), with roots of an upwelling plume at the core–mantle boundary (e.g., Rost et al., 2005). However, the exact dimensions and trajectory of the plumes through the mantle are debated, and greater complexity has been suggested. Precise imaging is challenging given the hypothesised narrow size of the plumes (Morgan, 1972) in comparison with the wavelengths of the seismic waves to image these features. For instance, plume ascent might not be vertical, perhaps deflected by mantle wind (Steinberger and O'Connell, 1998), and the dimensions of the plume might change from the lower mantle to the upper mantle (e.g., Richards et al., 1989; Tosi and Yuen, 2011). Due to a significant decrease in sensitivity, seismic anomalies associated with a certain temperature anomaly are also vastly decreased in the lower mantle, hampering reliable tracking of a seismic anomaly from the upper mantle through the transition zone into the lower mantle. And in turn, the exact relationship of the plume ascent in the lower mantle to the upper mantle is not well-understood. This is where mapping variations in mantle transition zone (TZ) thickness are useful. Elevated plume temperatures are predicted to deepen the 410- and shallow the 660-km depth mantle discontinuities thinning the transition zone (e.g., Deuss et al., 2013).

Hawaii is the archetypal example of hotspot volcanism. Low seismic velocities (and thus by proxy high thermal anomalies)

* Corresponding author at: National Oceanography Centre, University of Southampton, Waterfront Campus, European Way, Southampton SO14 3ZH, United Kingdom.
E-mail address: matthew.agius@soton.ac.uk (M.R. Agius).

http://dx.doi.org/10.1016/j.epsl.2017.06.033

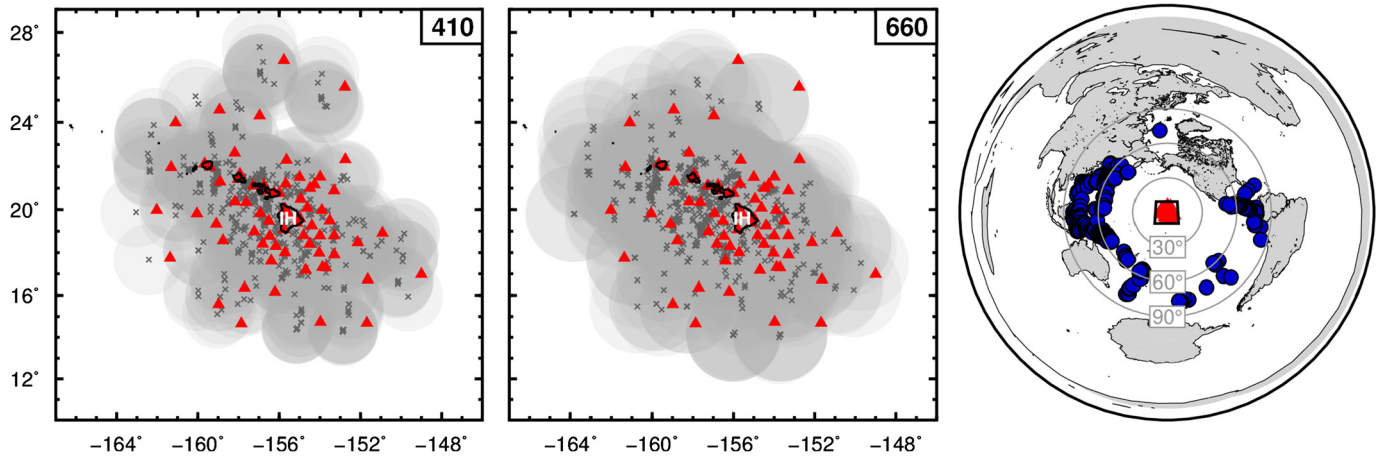

Fig. 1. Maps showing the distribution of piercing points at 410-km depth (left frame) and 660-km depth (central frame), and the corresponding stations (triangles) and earthquake sources (closed blue circles, right frame) used in this study. In the left two frames, semi-transparent grey shades are the corresponding Fresnel sensitivity zone for each piercing point. In the right frame, concentric circles show epicentral distance away from the study area. IH: Island of Hawaii.

have been imaged in the uppermost mantle beneath Hawaii (e.g., Laske et al., 2011), extending into the lower mantle (Wolfe et al., 2009, 2011; Cheng et al., 2015), and possibly down to the core–mantle boundary (e.g., Lei and Zhao, 2006; French and Romanowicz, 2015). Measurements for the mantle transition zone thickness using seismic receiver functions (RF) show areas that have considerable thinning and other areas with significant thickening (e.g., Li et al., 2000). A thinned transition zone has been located beneath different areas, with different thicknesses and lateral dimensions. For example, a thinner transition zone has been identified west–southwest of the Hawaiian islands, (Li et al., 2000; Collins et al., 2002), beneath the islands (Shen et al., 2003), and east of Hawaii close to the Island of Hawaii (Huckfeldt et al., 2013). It is unclear whether the main topographic contribution for the thinned TZ is from an updoming of the 660-km discontinuity (Li et al., 2000), a depressed 410, or a combination of a depressed 410 and an updoming 660 (Wölbern et al., 2006; Huckfeldt et al., 2013). Seismic tomographic images of a deflected plume within the TZ have been interpreted to be vertically tilted SE–NW (Wolfe et al., 2009; Cheng et al., 2015) and SW–NE (Wölbern et al., 2006). Each of these possibilities has geodynamic implications as to whether a plume is ponding below, within, or above the transition zone, and also has implications on the trajectory of the plume to the surface. It is thus essential for our understanding to discriminate between these possibilities. Here we use P-to-S receiver functions determined from ocean bottom seismometers (OBSs) and permanent land stations to image variations in the 410- and 660-km depth discontinuities beneath Hawaii and constrain the trajectory and dimensions of the plume. We apply improved signal processing techniques on the OBS data to enhance signal to noise and enhance imaging across the region.

2. Data and method

We made use of publicly available data from a combination of permanent and temporary, land and ocean-bottom broadband seismometers across the Hawaiian archipelago. Many of the stations have been deployed at different times through different projects such as the Hawaiian Plume–Lithosphere Undersea Mantle Experiment (PLUME, Laske et al., 2009, 2011) and the Ocean Seismic Network Pilot Experiment (OSNPE site OSN-1, Collins et al., 2001). Waveforms of teleseismic earthquakes with a magnitude greater than $M_w = 5.5$ and with an epicentral distance to the stations between 35° and 80° were downloaded from the Incorporated Research Institutions for Seismology (IRIS) data management centre. The seismic stations and earthquakes used in this study are shown in Fig. 1. The earthquakes are listed in Supplementary Table 1.

Preprocessing of the waveforms included: decimating the seismograms to 10 samples per second, band-pass filtering between 0.05–0.2 Hz, and rotating the horizontal components to the radial and transverse components using orientation corrections determined from the polarization of teleseismic surface waves (Rychert et al., 2013). Where unavailable, orientations were determined from P-wave polarization analysis. The chosen frequency range for the filtering was selected following tests on the data for both land and ocean stations. Supplementary Fig. 1 shows examples of different frequency ranges tested. Additional preprocessing to the ocean stations included the removal of tilt noise on the vertical components (Crawford and Webb, 2000) and the removal of compliance noise, as a result of pressure variations associated with infra-gravity waves (Bell et al., 2015).

Each recorded earthquake was manually inspected and a distinct P-wave arrival within ±5 seconds of the theoretical arrival was selected. This signal was deconvolved from the radial component using the extended multitaper frequency domain deconvolution technique (Helffrich, 2006; Rychert et al., 2013) to produce a receiver function, which is essentially a band limited impulse response of a P-to-S (Ps) phase conversion as a result of a seismic velocity discontinuity located beneath the station. The deconvolution effectively removes the effects of the instrument response and source spectra. A positive amplitude RF phase indicates a velocity increase with depth, whereas a negative amplitude indicates a velocity decrease. Data from OBS stations have higher noise levels, as expected, and thus require careful selection. We inspected each RF, eliminated unstable deconvolutions (pure ringing), and only selected cases with a clear Ps phase amplitude of $\gtrsim 0.2$ for the Moho discontinuity and $\gtrsim 0.1$ for 410 and 660 discontinuities (P410s and P660s, respectively). Theoretical arrival times of the three Ps phases acted as a guide for the selected arrival time.

In practice, a strong Moho phase was generally present in the RFs. However, given that P410s and P660s conversions arrive far into the coda, it was common that one phase was clear, while the other was obscured by ringing. In an effort to maximise the potential use of as many waveforms as possible, individual data sets were selected for the P410s and the P660s. These waveforms had to have a good Moho phase and a good signal for the respective phase. In an interactive process, the P wave was re-examined and the receiver function reviewed where necessary.

Each receiver function is migrated to depth, correcting for the sphericity of the Earth. We use a crust-corrected, one-dimensional